minerals

Article

Second Natural Occurrence of $KFeS_2$ (Hanswilkeite): An Inclusion in Diamond from the Udachnaya Kimberlite Pipe (Siberian Craton, Yakutia)

Alla M. Logvinova [1,*] and Igor S. Sharygin [1,2]

[1] V. S. Sobolev Institute of Geology and Mineralogy, Siberian Branch of the Russian Academy of Sciences, Koptyuga Pr. 3, Novosibirsk 630090, Russia; isharygin@crust.irk.ru
[2] Institute of the Earth's Crust, Siberian Branch of the Russian Academy of Sciences, Lermontova St. 138, Irkutsk 664033, Russia
* Correspondence: logv@igm.nsc.ru

Abstract: Potassium sulfide $KFeS_2$ (hanswilkeite) has been identified in polymineralic inclusions in a diamond from the Udachnaya kimberlite pipe (Siberian craton, Yakutia). This is the second occurrence of hanswilkeite in nature and the first one in mantle-derived samples. Sulfide $KFeS_2$ is monoclinic, the space group—C 2/c. Its crystal structure consists of chains with K in the interstices. The tetrahedra are centered by iron ions and linked by edges, thus forming chains of $[FeS_2]$ frameworks. The strongest lines of the electron diffraction powder pattern are 7.05 Å—(200); 5.34 Å ($0\bar{2}0$); and 3.05 Å ($2\bar{2}0$), and the angles between directions are $<2\bar{2}0/0\bar{2}0>$—60° and $<2\bar{2}0/200>$—30°. $KFeS_2$ has been found as a discrete phase within polymineralic inclusions consisting of apatite, ilmenite, chondrodite, phlogopite, dolomite, and a fluid phase. The data obtained from the composition of the hanswilkeite ($KFeS_2$) inclusion and other rare minerals (chondrodite, Mg-apatite, Cr-ilmenite) in primary inclusions in a diamond from the Udachnaya kimberlite testify to the important role of metasomatic processes in diamond formation.

Keywords: diamond; potassium sulfide; inclusion; kimberlite; mantle; craton

check for updates

Citation: Logvinova, A.M.; Sharygin, I.S. Second Natural Occurrence of $KFeS_2$ (Hanswilkeite): An Inclusion in Diamond from the Udachnaya Kimberlite Pipe (Siberian Craton, Yakutia). *Minerals* **2023**, *13*, 874. https://doi.org/10.3390/min13070874

Academic Editor: Fanus Viljoen

Received: 24 May 2023
Revised: 21 June 2023
Accepted: 23 June 2023
Published: 28 June 2023

1. Introduction

Sulfides are widespread mineral inclusions in diamonds [1–4]. They provide significant information about Earth's mantle and have been the subject of intensive studies during many years [1–7]. The abundance of sulfide as inclusions in diamonds and their intergrowth with syn-/protogenetic mantle silicates (olivine, orthopyroxene, clinopyroxene, and pyrope) in diamonds suggest that inclusions of sulfide are also syn-/protogenetic. Sulfides in diamond inclusions are represented by pyrrhotite, pentlandite, troilite, chalcopyrite, pyrite, djerfisherite, and monosulfide solid solutions [8]. Similar to silicate assemblages in diamonds, sulfide inclusions also belong to two types of mantle paragenesis: eclogitic (Ni-poor, 0–12 wt% Ni) and peridotitic (Ni-rich, 22–36 wt% Ni) [1,4]. Thus, sulfides are thought to be present in growth environments of diamonds.

Sulfides have also been described in nanometer-sized (submicron) polymineral inclusions in fibrous diamonds [9,10]. These inclusions represent well-preserved samples of diamond-forming media and appear to represent originally homogeneous phases (melts or high-density fluids) entrapped by the growth of the fibrous diamonds at depths > 4 GPa. Subsequently, these trapped melts or fluids crystallized into a range of daughter minerals and fluid phase(s). Sulfides in such inclusions are represented by chalcopyrite $CuFeS_2$, pentlandite $(Fe,Ni)_9S_8$, heazlewoodite Ni_3S_2, pyrrhotite $Fe_{1-x}S$, and troilite FeS, as well as unidentified sulfides of Cu and Ni. Moreover, energy-dispersive spectra of some Fe-rich sulfide phases in nanometer-sized polymineralic inclusions showed a stable presence of potassium [9]. However, K-containing sulfides were not reliably identified.

Currently, five potassium-bearing sulfides are approved as mineral species by the International Mineralogical Association (IMA): murunskite $K_2(Cu,Fe)_4S_4$, rasvumite KFe_2S_3, djerfisherite $K_6(Fe,Cu,Ni)_{25}S_{26}Cl$, bartonite $K_6Fe_{20}S_{26}S$, chlorbartonite $K_6Fe_{24}S_{26}Cl$, and hanswilkeite $KFeS_2$ [11–19]. $KFeS_2$ has been known since 1869. Crystals of $KFeS_2$ were obtained from the reaction of a mixture of potassium carbonate, iron, and sulfur, followed by extracting the solidified melt with water. The structure was first determined in 1942 by Boon and MacGillavry [20,21]. $KFeS_2$ is not oxidized in air and it is resistant to water, and thus it is a stable phase in laboratory experiments [22]; however, until recently, it has not been known as a naturally occurring mineral. In 2022, $KFeS_2$ was recognized by the IMA as a new mineral—hanswilkeite (IMA no. 2022-041) [19]. Hanswilkeite was found in fine-grained tilleite–calcite marble, often intergrown with rasvumite, in association with pyrite and oldgamite [S.N. Britvin, personal communication]. The size of its discharge is up to 1 mm.

In this paper, we, for the first time, identified potassium sulfide $KFeS_2$ (potassium thioferrite) in nanometer-sized polymineralic inclusions in a diamond from the Udachnaya kimberlite pipe (Siberian craton, Yakutia).

2. Materials and Methods

The studied diamond (sample no. Ud-45) is a cubic crystal with a fibrous inner structure and dark cloud of numerous nanometer-sized polymineralic inclusions in its central part (Figure 1a).

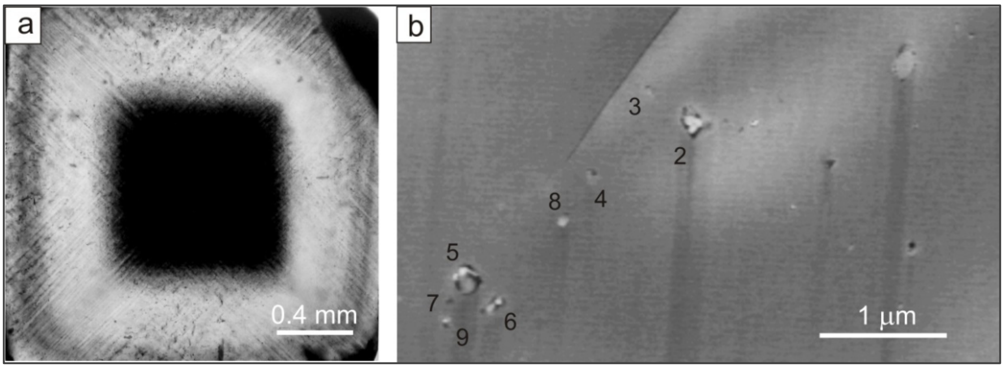

Figure 1. Optical micrograph of the cubic diamond Ud-45 from Udachnaya kimberlite pipe (**a**); TEM bright field image of nanometer-sized inclusions in diamond (**b**). The numbers indicate the location of the studied inclusions.

Microstructures and compositional features of phases in polymineralic inclusions in diamond Ud-45 were identified with the transmission electron microscope (TEM) Tecnai G2 F20 X-Twin operated at 200 kV with a Schottky emitter as an electron source (FEG) at GeoForschungsZentrum (GFZ), Potsdam, Germany. The diamond crystal was polished parallel to (110) on both sides to make a 1 mm thick plate (Figure 1a). Electron-transparent foils with typical dimensions of 15 µm × 8 µm × 0.15 µm were prepared, applying focused ion beam (FIB) sample preparation. Details of the foil preparation are given in [23,24]. The TEM was equipped with an EDAX X-ray analyzer with an ultra-thin window, a Fishione high-angle annular dark-field (HAADF) detector, and a Gatan imaging filter (Tridiem, Richmond, VA, USA) for electron energy-loss spectroscopy and energy filtered imaging. HAADF images were collected with a camera length of 330 mm displaying a diffraction contrast plus a Z-contrast or with a camera length of 75 mm, which shows a Z-contrast only. Nanophases were identified by acquiring high-resolution lattice fringe images with a short acquisition time (0.6 s) to avoid decomposition during exposure to the electron beam [24]. The calculated diffraction patterns (using the Fast Fourier Transform (TEM)) from high-resolution images were used to measure d-spacing and angles between the adjacent lattice planes. A comparison of the observed data with calculated data from known phases (literature data) allowed for identifying the phases present. The chemical composition of the phases was always measured in the scanning transmission mode (STEM), thus avoiding a significant mass loss during data acquisition. The acquisition time was 60 or 120 s.

3. Results and Discussion

Twelve separate polymineralic inclusions ranging from 100 to 700 nm in size were studied in the diamond Ud-45 (Figure 2). The inclusions show negative crystal shapes with parallel facets (Figure 3). They are not related to any healed cracks. Therefore, they may be considered as primary/fluid inclusions (i.e., those that form while crystals are growing).

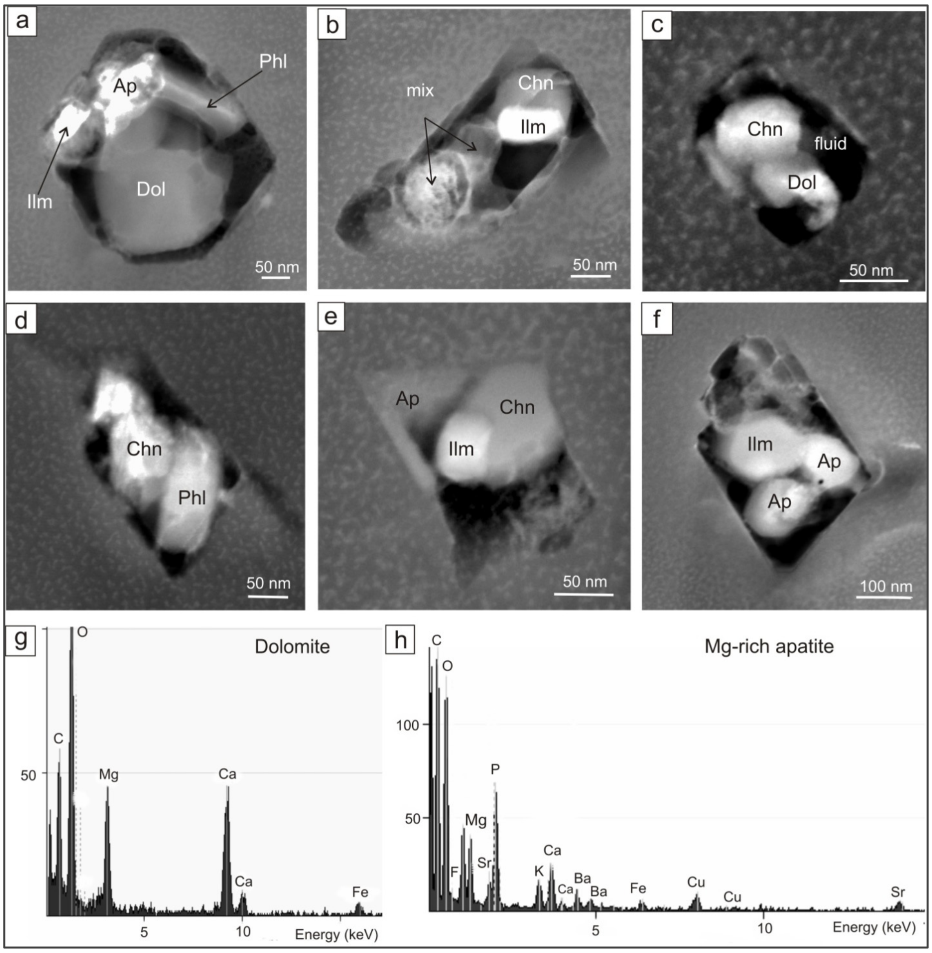

Figure 2. TEM images of nanometer-sized polymineralic inclusions in diamond Ud-45 (**a**–**f**): Ap—apatite, Ilm—ilmenite, Chn—chondrodite, Dol—dolomite, Phl—phlogopite; (**g**,**h**)—EDX spectra of dolomite and apatite (Cu intensity comes from the copper grid).

The daughter phase assemblages are represented by silicate, carbonate, phosphate, oxide, and chloride minerals. There are voids inside inclusions that likely are filled by the fluid phase. The main minerals are dolomite, chondrodite (a member of the humite group: (Mg, Fe^{2+})$_5$(SiO_4)$_2$(F,OH)$_2$)), phlogopite, Mg-rich apatite, Cr-bearing ilmenite, magnetite, K-Fe-sulfide, and KCl (Figures 2 and 3). Dolomite was recognized as the dominant phase in the inclusions. The next most common phases are silicates: phlogopite and chondrodite.

Chondrodite has not yet been reported as an inclusion in a diamond. This silicate was identified using diffraction patterns. All measured *hkl* values of the studied chondrodite were compared with the calculated ones for interplanar distances of the reference $Mg_5(SiO_4)_2(F,OH)_2$ (Table 1). The chondrodite phases within polymineralic inclusions are characterized by Ti impurity (Figure 3A,E).

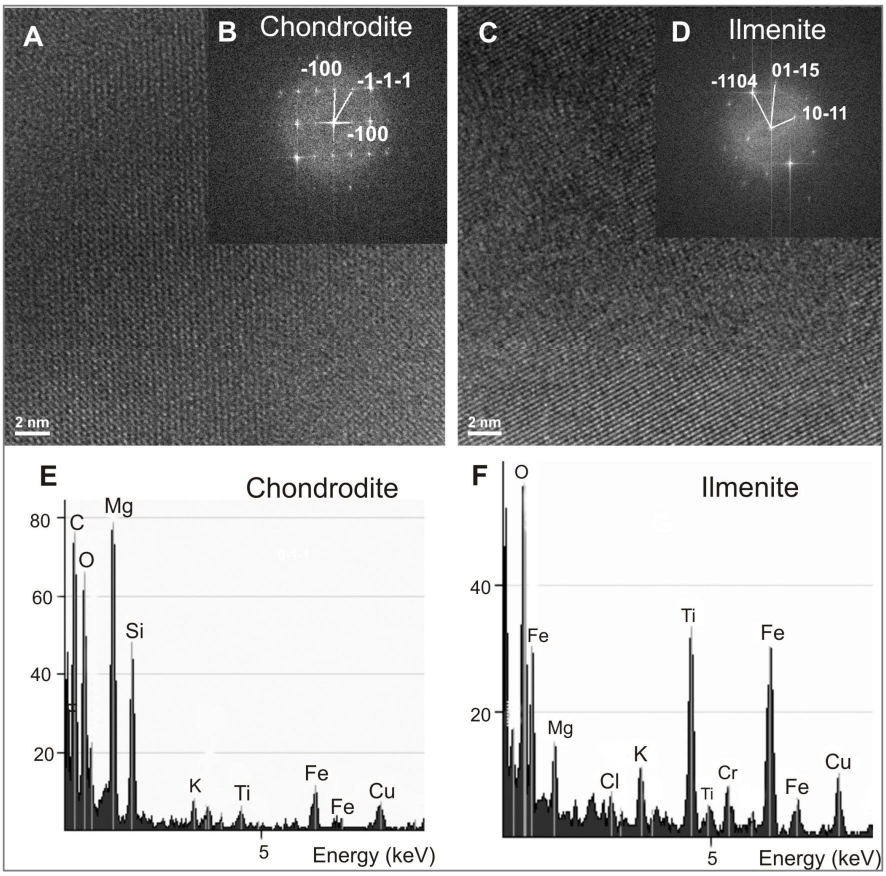

Figure 3. Energy filtered lattice fringe images and diffraction patterns (FFT) from the framed area of two nanometric phases in polymineral inclusion #6 (see Figure 1b) from the diamond Ud-45: (**A**,**B**)—chondrodite; (**C**,**D**)—ilmenite. (**E**,**F**) X-ray intensity spectrum of nanometric phases: (**E**) chondrodite and (**F**) ilmenite. Cu intensity comes from the copper grid.

Table 1. Interplanar distances and angles between planes with electron diffraction of nanometer-sized phases of chondrodite and $KFeS_2$ in diamond Ud-45.

hkl	d_{hkl} **Observed, Å**	d_{hkl} **Calculated, Å**	**φ ***	$\varphi_{observed}$, **Degrees**	$\varphi_{calculated}$, **Degrees**
			Chondrodite		
$\bar{1}00$	7.37	7.432			
$0\bar{1}\bar{1}$	4.18	4.251			
$\bar{1}\bar{1}\bar{1}$	3.58	3.481			
			$\langle\bar{1}\bar{1}\bar{1}/0\bar{1}\bar{1}\rangle$	28.5	27
			$\langle\bar{1}\bar{1}\bar{1}/\bar{1}00\rangle$	57	54.1
			$KFeS_2$		
200 (100)	7.05 (3.535)	7.022 (3.511)			
$0\bar{2}0$	5.34	5.644			
$2\bar{2}0$	3.05	2.816			
			$\langle 2\bar{2}0/0\bar{2}0\rangle$	60	61
			$\langle 2\bar{2}0/200\rangle$	30	30

Note: * φ—angle between planes.

The porous microstructure of the polymineralic inclusions requires the presence of a fluid phase during the formation of the inclusion, which has been partly released during FIB sample preparation (Figure 2). For simplicity, these decrepitated fluid inclusions are labeled "fluid" in the figures.

A total of 21 phases in 12 individual polymineralic nanoinclusions were analyzed. For the smallest phases after imaging with high-resolution electron microscopy (HREM), the compositional measurements were carried out using a defocused beam. It turned out to be extremely important to defocus the beam (the size of the focusing spot is about 0.1 nm) in order to avoid a mass loss during the measurement. This was achieved by expanding the beam to the diameter of nanocrystals (about 20–30 nm). Crystal structure data of the minerals within nanoinclusions were derived from selected area diffraction patterns (Figure 3) and from Fast Fourier Transforms (FFT), which were calculated from energy-filtered high-resolution images using the Gatan Digital Micrograph software package version 3.5. The main emphasis was placed on the study of the $FeKS_2$ phase.

The largest sulfide grain of a potassium iron sulfide was found in inclusion #6 that abuts a void, formerly filed by a fluid phase (Figure 4). Its diameter is about 50 nm. The nanoinclusion of sulfide is mainly composed of potassium, iron, and sulfur. It was identified by EDX spectra with a very intense peak of K, Fe, and S (Figure 4E). The weak X-ray intensities of Cu–Kα in the spectrum are due to the copper grid.

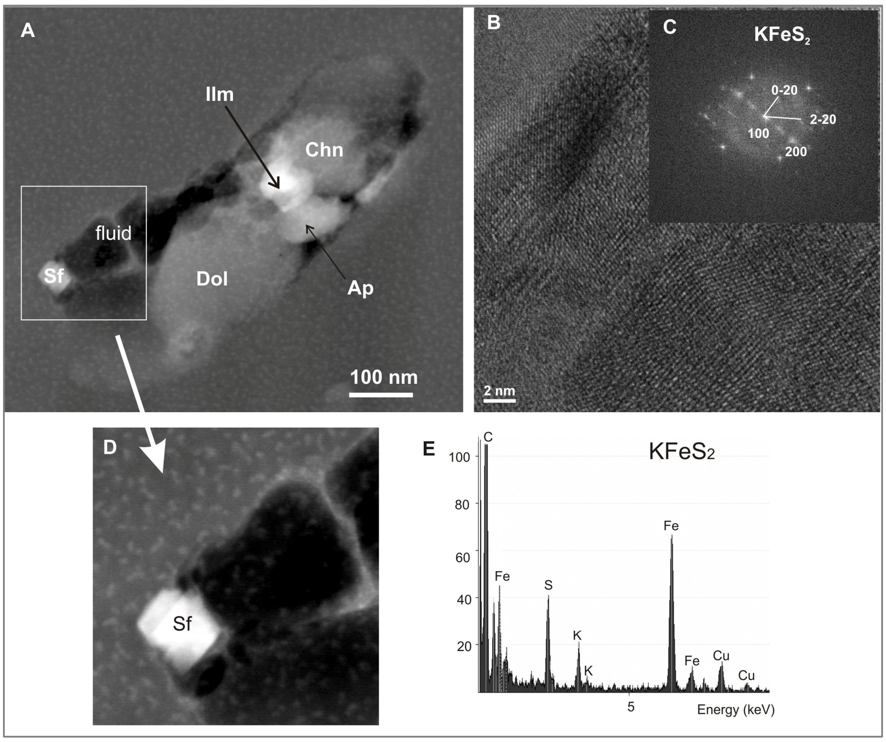

Figure 4. TEM bright field image of nanometer-sized inclusion #6 (see Figure 1b) from the diamond Ud-45 (**A**): Ap—apatite, Ilm—ilmenite, Chn—chondrodite, Dol—dolomite, Sf—sulfide $KFeS_2$; (**B**)—energy filtered high-resolution (HREM) lattice fringe image of sulfide $KFeS_2$. (**C**) Diffraction pattern (FFT) from framed area in $KfeS_2$. The spacing between the fringes is used for phase identification. (**D**)—Enlarged fragment of TEM image of sulfide inclusion $KFeS_2$. (**E**)—Energy-dispersive X-ray (EDX) spectra of sulfide $KFeS_2$. Cu intensity comes from the copper grid.

Further identification of the K-Fe-sulfide was performed with diffraction measurements (Figure 4B,C). The d_{hkl} values obtained for the studied K-Fe-sulfide match well with those of the synthetic reference $KFeS_2$ [20,21].

According to [21], the crystal structure of the synthetic phase $KFeS_2$ is monoclinic with the cell parameters a_o = 7.05 Å; b_o = 11.28 Å; and c_o = 5.39 Å. The space group of $KFeS_2$ is C 2/c.

All measured d_{hkl} distances obtained from the HREM images and from the electron diffraction patterns of the selected areas, compared with the synthetic $FeKS_2$ data, are presented in Table 1. This table also lists data on the silicate phase of chondrodite, which is present in these polymineralic inclusions.

The first column lists the Miller indices (*hkl*), which are used to label the planes. The second column displays the d_{hkl} values observed from the electron diffraction pattern. The third column shows the data d_{hkl} calculated from HREM results. The lattice parameters are very close. All calculations of distances and angles between planes (φ) were carried out using the Desktop Microscopy software package version 2.1. [21].

The angles between the planes, indicated in Table 1, in the case of $KFeS_2$ were also recalculated one by one, applying the program "Single Crystal" using the zone axis [002] derived from the diffraction pattern. The angles are the same.

The diffraction data and the cell constants of the $KFeS_2$ obtained are shown on the projection of the crystal lattice along the *z*-axis (Figure 5).

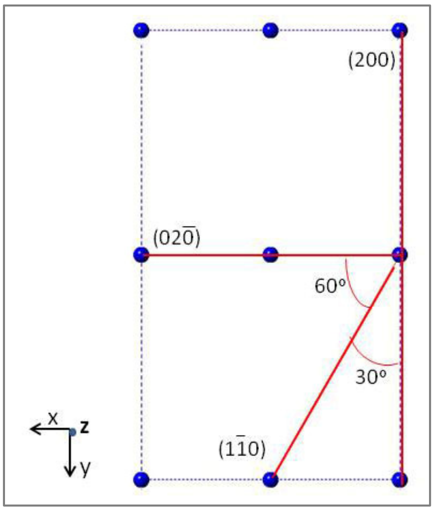

Figure 5. Projection of the crystal lattice of $KFeS_2$ along the *z*-axis.

The crystal structure of the $KFeS_2$ phase in the inclusions was plotted using the Crystal Maker 2.7.3 program and is shown in Figure 6. It consists of chains with K in the interstices. Iron occupies the centers of the tetrahedra and is surrounded by S. These tetrahedra are centered by iron ions and linked by edges, thus forming chains of L[FeS_2] (Figure 6). Such an arrangement fits the symmetry conditions of the space group C 2/c very well. Placing the eight S atoms in general positions, we can calculate the parameter values, which lead to the arrangement illustrated in Figure 6.

Submicron polymineralic inclusions in fibrous diamonds (including cuboid, coated, and cloudy varieties) are snapshots of (metasomatic) fluids or melts from which the diamonds grew [9,10,25,26]. The described multiphase assemblage of such inclusions represents a set of daughter phases of an originally homogenous liquid phase called high-density fluid (HDF), which is similar to supercritical fluids or melts enriched with volatile components [26]. The bulk compositions of submicron inclusions in fibrous diamonds widely vary between three general end-members: (i) a silicic end-member rich in Si, Al, water, and alkalis; (ii) a saline end-member rich in Cl, water, and alkalis; and (iii) a carbonatitic end-member rich in CO_2, Mg, Ca, and alkalis [26–33]. The daughter phase assemblage of the inclusions in the diamond Ud-45 is dolomite > chondrodite and phlogopite > Mg-rich apatite, Cr-bearing ilmenite, magnetite, K-Fe-sulfide ($KFeS_2$) and sylvite. This indicates that a melt/fluid entrapped in the studied diamond Ud-45 is carbonatitic or silicate–carbonate in composition with high potassium and volatile contents.

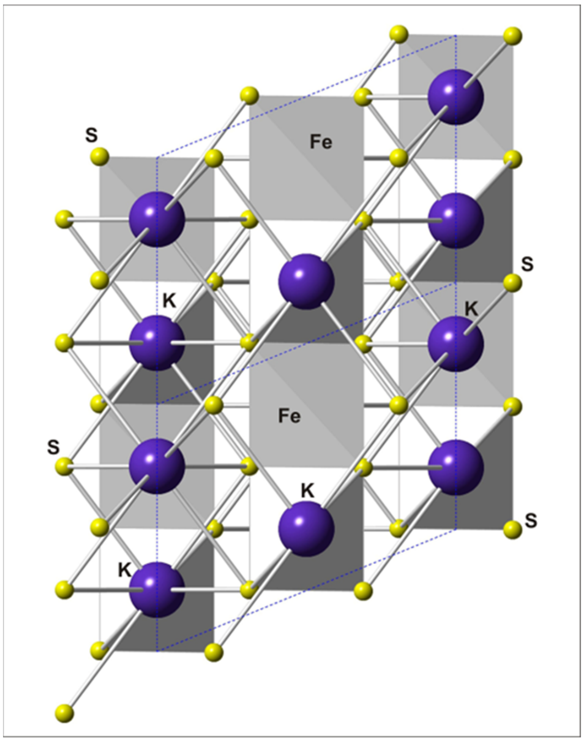

Figure 6. Crystal structure of mineral phase $KFeS_2$ in the diamond Ud-45. Projection is along the [010] direction. Interatomic distances: K-S—3.38–3.45 Å (eight-fold coordination) and Fe-S—2.18–2.19 Å (tetrahedral coordination).

The $KFeS_2$ compound has previously been reported as a naturally occurring mineral at low pressures. $KFeS_2$ reported here as an inclusion in a diamond is the first discovery in high-pressure natural materials. Experimental studies of a complex K-Fe-S system are limited by 300–600 °C and ambient pressure [34]. This study predicted that the formation of $KFeS_2$ in nature is possible, but it requires either extremely high potassium activity or high sulfur fugacity (Figure 7) [34]. Such conditions could be realized inside the inclusions in the studied diamond Ud-45 during the freezing of the melt/fluid.

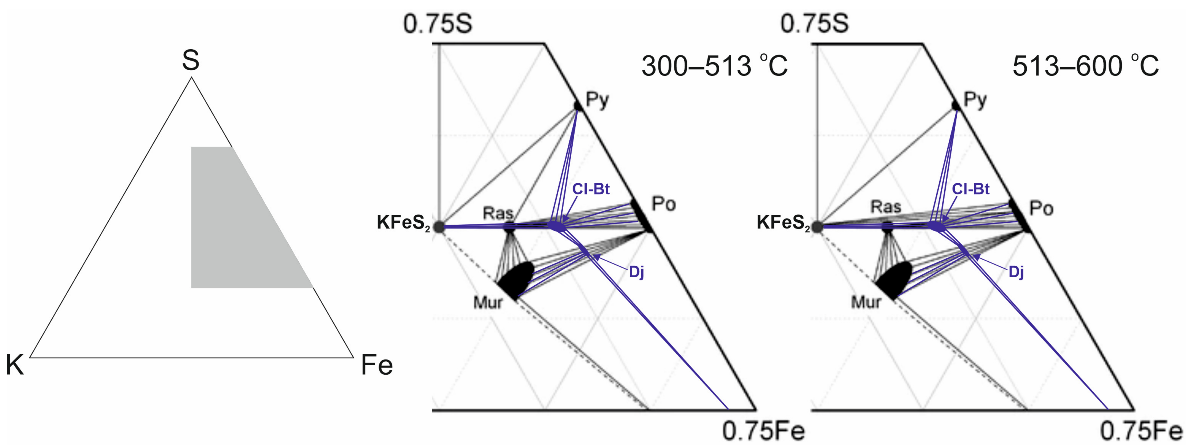

Figure 7. K–Fe–S–Cl phase diagram presented by Osadchii et al. (2018) [34]. Black color shows the phase relations experimentally obtained in the K–Fe–S system at 300–600 °C [34]. Blue color shows the phase relations including chlorbartonite and djerfisherite. Py—pyrite, Po—pyrrhotite, Ras—rasvumite, Mur—murunskite, Ch-Bt—chlorbartonite, Dj—djerfisherite.

4. Conclusions

(1) The daughter phase assemblage of the polymineralic inclusions (i.e., the crystallized mantle melt/fluid) in the cubic fibrous diamond Ud-45 from the Udachnaya kimberlite pipe is represented by dolomite, chondrodite, phlogopite, Mg-rich apatite, Cr-bearing ilmenite, magnetite, hanswilkeite ($KFeS_2$), KCl, and fluid. The melt/fluid is likely carbonatitic or silicate–carbonate in composition with high potassium and volatile contents.

(2) For the first time, potassium sulfide hanswilkeite $KFeS_2$ and chondrodite have been found in a diamond as a mineral reflecting mantle substrates.

Author Contributions: Conceptualization, A.M.L. and I.S.S.; investigation, A.M.L.; data curation, A.M.L. and I.S.S.; writing—original draft preparation, A.M.L.; writing—review and editing, I.S.S.; visualization, A.M.L. and I.S.S.; funding acquisition, I.S.S. All authors have read and agreed to the published version of the manuscript.

Funding: This work was financially supported by the Russian Science Foundation (grant no. 18-77-10062-P) and state assignment of IGM SB RAS (no. 122041400157-9).

Data Availability Statement: Not applicable.

Acknowledgments: The authors are very grateful to Richard Wirth for the research carried out on the TEM at the Helmholtz Center Potsdam GFZ German Research Center for Geosciences (Germany) with unique results. We also express our gratitude to Yu.V. Seretkin (IGM SB RAS, Novosibirsk, Russia) for help in constructing projection images using special software.

Conflicts of Interest: The authors declare no conflict of interest.

References

1. Bulanova, G.P.; Shestakova, O.E.; Leskova, N.V. Djerfisherite from Sulfide Inclusions in Diamond. Yakutia. *Dokl. Earth Sci.* **1980**, *255*, 430–433.
2. Sharp, W.E. Pyrrhotite, a common inclusion in South African diamonds. *Nature* **1966**, *211*, 402–403. [CrossRef]
3. Sobolev, N.V.; Yefimova, E.S.; Logvinova, A.M.; Sukhodol'skaya, O.P.; Solodova, Y.P. Abundance and composition of mineral inclusions in large diamonds from Yakutia. *Dokl. Earth Sci.* **2001**, *376*, 34–38.
4. Yefimova, E.S.; Sobolev, N.V.; Pospelova, L.N. Sulfide inclusions in diamonds and features of their parageneses. *Zap. Vses. Mineral. Ova.* **1983**, *112*, 300–310.
5. Deines, P.; Harris, J.W. Sulfide inclusion chemistry and carbon isotopes of African diamonds. *Geochim. Cosmochim. Acta* **1995**, *59*, 3173–3188. [CrossRef]
6. Harris, J.W. Black material on mineral inclusions and in Internal fracture planes in diamond. *Contrib. Mineral. Petrol.* **1972**, *35*, 22–33. [CrossRef]
7. Pearson, D.G.; Shirey, S.B.; Harris, J.W.; Carlson, R.W. Sulphide inclusions in diamonds from the Koffiefontein kimberlite, S Africa: Constraints on diamond ages and mantle Re-Os systematics. *Earth Planet. Sci. Lett.* **1998**, *160*, 311–326. [CrossRef]
8. Taylor, L.A.; Liu, Y. Diamond sulfide inclusions are not Mss: Exsolution of pyrrhotite, pentlandite and chalcopyrite. *Russ. Geol. Geophys.* **2009**, *50*, 1201–1211. [CrossRef]
9. Logvinova, A.M.; Wirth, R.; Fedorova, E.N.; Sobolev, N.V. Nanometer-sized mineral and fluid inclusions in cloudy Siberian diamonds: New insights on diamond formation. *Eur. J. Miner.* **2008**, *20*, 317–331. [CrossRef]
10. Logvinova, A.M.; Wirth, R. Black cluster microinclusions in the core of Yakutian diamonds: Implications for diamond nucleation. In Proceedings of the 10th International Workshop "Deep Seated Magmatism, Its Sources and Plumes", Irkutsk, Russia; 2010; pp. 93–103.
11. Dobrovol'Skaya, M.G. Murunskite, $K_2Cu_3FeS_4$, a new sulfide of potassium, copper, and iron. *Int. Geol. Rev.* **1982**, *24*, 1109–1114. [CrossRef]
12. Pekov, I.V.; Zubkova, N.V.; Lisitsyn, D.V.; Pushcharovsky, D.Y. Crystal chemistry of murunskite. *Dokl. Earth Sci.* **2009**, *424*, 139–141. [CrossRef]
13. Sokolova, M.N.; Dobrovol'skaya, M.G.; Organova, N.I.; Dimitrik, A.L. A sulfide of iron and potassium, the new mineral rasvumite. *Zap. Vsesoyuznogo Mineral. Obs.* **1970**, *99*, 712–720.
14. Clark, J.R.; Brown, G.E. Crystal structure of rasvumite, KFe_2S_3. *Am. Mineral.* **1980**, *65*, 477–482.
15. Fuchs, L.H. Djerfisherite, alkali copper-iron sulfide: A new mineral from enstatite chondrites. *Science* **1966**, *153*, 166–167. [CrossRef]
16. Zaccarini, F.; Thalhammer, O.A.; Princivalle, F.; Lenaz, D.; Stanley, C.J.; Garuti, G. Djerfisherite in the Guli dunite complex, Polar Siberia: A primary or metasomatic phase? *Can. Mineral.* **2007**, *45*, 1201–1211. [CrossRef]

17. Czamanske, G.K.; Erd, R.C.; Leonard, B.F.; Clark, J.R. Bartonite, a new potassium iron sulfide mineral. *Am. Mineral.* **1981**, *66*, 369–375.
18. Yakovenchuk, V.N.; Pakhomovsky, Y.A.; Men'shikov, Y.P.; Ivanyuk, G.Y.; Krivovichev, S.V.; Burns, P.C. Chlorbartonite, $K_6Fe_{24}S_{26}$(Cl,S), a new mineral species from a hydrothermal vein in the Khibina massif, Kola Peninsula, Russia: Description and crystal structure. *Can. Mineral.* **2003**, *41*, 503–511. [CrossRef]
19. Murashko, M.N.; Britvin, S.N.; Krzhizhanoskaya, M.G.; Vereshchagin, O.S.; Vapnik, Y.; Vlasenko, N.S.; Shelukhina, Y.S.; Bocharov, V.N. Hanswilkeite, IMA-2022-041, in: CNMNC Newsletter 69. *Eur. J. Mineral.* **2022**, *34*, 463–468. [CrossRef]
20. Boon, J.W.; MacGillavry, C.H. The crystal structure of potassium thioferrite $KFeS_2$ and sodium thiochromite $NaCrS_2$. *Recl. Des Trav. Chim. Des Trav. Pays-Bas* **1942**, *61*, 910–920. [CrossRef]
21. Bronger, W.; Kyas, A.; Muller, P.J. The Antiferromagnetic Structures of $KFeS_2$, $RbFeS_2$, $KFeSe_2$, and $RbFeSe_2$ and the Correlation between Magnetic Moments and Crystal Field Calculations. *Solid State Chem.* **1987**, *70*, 262. [CrossRef]
22. Boller, H. On the synthesis, crystal chemistry and magnetic properties of rasvumite and related compound. *Acta Cryst.* **2004**, *60*, s47. [CrossRef]
23. Wirth, R. Focused ion beam (FIB): A novel technology for advanced application of micro- and nanoanalysis in geosciences and applied mineralogy. *Eur. J. Mineral.* **2004**, *16*, 863–877. [CrossRef]
24. Wirth, R. Focused Ion Beam (FIB) combined with SEM and TEM: Advanced analytical tools for studies of chemical composition, microstructure and crystal structure in geomaterials on a nanometre scale. *Chem. Geol.* **2009**, *261*, 217–229. [CrossRef]
25. Navon, O.; Hutcheon, I.D.; Rossman, G.R.; Wasserburg, G.J. Mantle-derived fluids in diamond micro-inclusions. *Nature* **1988**, *335*, 784–789. [CrossRef]
26. Gubanov, N.; Zedgenizov, D.; Sharygin, I.; Ragozin, A. Origin and Evolution of High-Mg Carbonatitic and Low-Mg Carbonatitic to Silicic High-Density Fluids in Coated Diamonds from Udachnaya Kimberlite Pipe. *Minerals* **2019**, *9*, 734. [CrossRef]
27. Schrauder, M.; Navon, O. Hydrous and carbonatitic mantle fluids in fibrous diamonds from Jwaneng, Botswana. *Geoch. Cosmochim. Acta* **1994**, *58*, 761–771. [CrossRef]
28. Klein-BenDavid, O.; Izraeli, E.S.; Hauri, E.; Navon, O. Fluid inclusions in diamonds from the Diavik mine, Canada and the evolution of diamond-forming fluids. *Geochim. Cosmochim. Acta* **2007**, *71*, 723–744. [CrossRef]
29. Klein-BenDavid, O.; Logvinova, A.M.; Schrauder, M.; Spetius, Z.V.; Weiss, Y.; Hauri, E.H.; Kaminsky, F.V.; Sobolev, N.V.; Navon, O. High-Mg carbonatitic microinclusions in some Yakutian diamonds—A new type of diamond-forming fluid. *Lithos* **2009**, *112*, 648–659. [CrossRef]
30. Zedgenizov, D.A.; Ragozin, A.L.; Shatsky, V.S. Compositional features of diamond growth medium: From the study of microinclusions in natural diamonds. *Proc. Russ. Miner. Soc.* **2007**, *7*, 159–172.
31. Zedgenizov, D.A.; Ragozin, A.L.; Shatsky, V.S.; Araujo, D.; Griffin, W.L.; Kagi, H. Mg and Fe-rich carbonate–silicate high-density fluids in cuboid diamonds from the Internationalnaya kimberlite pipe (Yakutia). *Lithos* **2009**, *112*, 638–647. [CrossRef]
32. Skuzovatov, S.Y.; Zedgenizov, D.A.; Ragozin, A.L.; Shatsky, V.S. Growth medium composition of coated diamonds from the Sytykanskaya kimberlite pipe (Yakutia). *Russ. Geol. Geophys.* **2012**, *53*, 1197–1208. [CrossRef]
33. Logvinova, A.; Zedgenizov, D.; Wirth, R. Specific Multiphase Assemblages of Carbonatitic and Al-Rich Silicic Diamond-Forming Fluids/Melts: TEM Observation of Microinclusions in Cuboid Diamonds from the Placers of Northeastern Siberian Craton. *Minerals* **2019**, *9*, 50. [CrossRef]
34. Osadchii, V.O.; Voronin, M.V.; Baranov, A.V. Phase equilibria in the $KFeS_2$–Fe–S system at 300–600 °C and bartonite stability. *Contrib. Mineral. Petrol.* **2018**, *173*, 44. [CrossRef]